International Journal of
Molecular Sciences

MDPI

Article

Locus Coeruleus Neurons' Firing Pattern Is Regulated by ERG Voltage-Gated K^+ Channels

Sonia Hasan [1,*], Francis Delicata [2], Leonardo Guasti [3], Claudia Duranti [4], Fatemah Mousalem Haidar [5], Annarosa Arcangeli [4], Paola Imbrici [6], Mauro Pessia [5,7], Mario Valentino [7] and Maria Cristina D'Adamo [8,*]

1 Department of Physiology, Faculty of Medicine, Kuwait University, Safat 13110, Kuwait
2 College of Pharmacy, Rady Faculty of Health Sciences, University of Manitoba, Winnipeg, MB R3E 0T5, Canada
3 Centre for Endocrinology, William Harvey Research Institute, Faculty of Medicine and Dentistry, Queen Mary University of London, London EC1M 6BQ, UK
4 Department of Experimental and Clinical Medicine, Section of Internal Medicine, University of Florence, 50121 Firenze, Italy
5 Department of Physiology, College of Medicine and Health Sciences, United Arab Emirates University, Al Ain 17666, United Arab Emirates
6 Department of Pharmacy—Drug Sciences, University of Bari "Aldo Moro", 70121 Bari, Italy
7 Department of Physiology & Biochemistry, Faculty of Medicine & Surgery, University of Malta, MSD 2080 Msida, Malta
8 Department of Medicine & Surgery, LUM University "Giuseppe Degennaro", Casamassima, 70010 Bari, Italy
* Correspondence: sonia.hasan@ku.edu.kw (S.H.); dadamo@lum.it (M.C.D.); Tel.: +39-3925645119 (S.H. & M.C.D.)

Abstract: Locus coeruleus (LC) neurons, with their extensive innervations throughout the brain, control a broad range of physiological processes. Several ion channels have been characterized in LC neurons that control intrinsic membrane properties and excitability. However, ERG (*ether-à-go-go–related gene*) K^+ channels that are particularly important in setting neuronal firing rhythms and automaticity have not as yet been discovered in the LC. Moreover, the neurophysiological and pathophysiological roles of ERG channels in the brain remain unclear despite their expression in several structures. By performing immunohistochemical investigations, we found that ERG-1A, ERG-1B, ERG-2 and ERG-3 are highly expressed in the LC neurons of mice. To examine the functional role of ERG channels, current-clamp recordings were performed on mouse LC neurons in brain slices under visual control. ERG channel blockade by WAY-123,398, a class III anti-arrhythmic agent, increased the spontaneous firing activity and discharge irregularity of LC neurons. Here, we have shown the presence of distinct ERG channel subunits in the LC which play an imperative role in modulating neuronal discharge patterns. Thus, we propose that ERG channels are important players behind the changes in, and/or maintenance of, LC firing patterns that are implicated in the generation of different behaviors and in several disorders.

Keywords: locus coeruleus neurons; noradrenergic system; ERG K^+ channels; *ether-à-go-go–related gene*; WAY-123,398; class III anti-arrhythmic drug

Citation: Hasan, S.; Delicata, F.; Guasti, L.; Duranti, C.; Haidar, F.M.; Arcangeli, A.; Imbrici, P.; Pessia, M.; Valentino, M.; D'Adamo, M.C. Locus Coeruleus Neurons' Firing Pattern Is Regulated by ERG Voltage-Gated K^+ Channels. *Int. J. Mol. Sci.* **2022**, *23*, 15334. https://doi.org/10.3390/ijms232315334

Academic Editor: Dax A. Hoffman

Received: 11 June 2022
Accepted: 2 December 2022
Published: 5 December 2022

1. Introduction

Located in the anterior pons, the locus coeruleus (LC), with its extensive innervations throughout the central nervous system, is the major noradrenergic nucleus of the brain and thereby controls a broad range of physiological processes that include cognition, learning and memory, sleep–wake cycle, arousal, attention, mood, anxiety and pain [1–7]. These and other neurophysiological processes are known to be affected by changes in the discharge properties of LC neurons [7], which in turn are dependent on the intrinsic membrane properties and the ion channel constituents of these neurons. For example, in a previous study, we demonstrated that the inwardly rectifying potassium channel

Kir5.1 plays a crucial role in defining the CO_2/pH sensitivity of LC neurons. The LC is a CO_2-chemosensitive region of the pons where more than 80% of its neurons respond to hypercapnic acidosis with an increase in firing rate [8,9]. Kir5.1 is likely a key contributor to LC's firing response to hypercapnic acidosis [8].

LC neurons are endogenous pacemakers that fire spontaneous and repetitive action potentials [9]. Besides Kir5.1, several ion channels have been characterized in LC neurons [8,10–15]. However, ERG (*ether-à-go-go–related gene*) channels that belong to the KCNH super-family of K^+ channels [16], and that are particularly important in setting neuronal firing rhythms and automaticity [16–18], have not been identified thus far in the LC. ERG channels can be subdivided into three groups: ERG-1 (*KCNH2*, Kv11.1), ERG-2 (*KCNH6*, Kv11.2) and ERG-3 (*KCNH7*, Kv11.3). In addition, a long splice variant of ERG-1 (ERG-1A) and a short one (ERG-1B) have been identified [19]. ERG channels have been implicated in the regulation of excitability, discharge pattern, spike-frequency adaptation and the resonance properties of neurons [17,18,20,21].

The human ERG-1 (hERG-1; *KCNH2*) encodes the pore-forming subunit of a rapid-delayed rectifier K^+ channel, the current (I_{Kr}) through which ensures a fast repolarization phase of the cardiac action potentials and, consequently, regulates heart rhythms [22]. Its dysfunction is known to cause *long QT syndrome* and inherited and acquired cardiac arrhythmias [22,23]. However, while the role of this channel is quite well-established in cardiomyocytes, in the central nervous system its neurophysiological and pathophysiological roles remain unclear despite its expression in several crucial brain structures [18–20,24–28].

By performing immunohistochemical and electrophysiological investigations, we found that ERG-1A, ERG-1B, ERG-2 and ERG-3 are highly expressed in LC neurons, where members of the ERG channel family modulate intrinsic electrical properties and rhythmic firing.

2. Results

2.1. Immunohistochemical Localization of ERG Channels within Murine LC Nuclei

In order to determine the localization of ERG channel types within the LC nuclei, rabbit polyclonal anti-ERG-1A, anti-ERG-1B, anti-ERG-2 and anti-ERG-3 antibodies were produced, purified and tested as previously described [19]. Using these antibodies, positive immunoreactivity was observed within the brainstem slices that were dissected from C57BL/6J mice. LC neurons were stained with the anti-ERG-1A, anti-ERG-1B, anti-ERG-2 and anti-ERG-3 antibodies and the signal was highly specific (Figure 1A–E). Notably, the images point out that numerous cell bodies located within the LC nucleus were immunopositive for all channel types. As reported for other brain regions [19,20], ERG-2 appeared to be the least expressed among the channel subfamily. For ERG-1A and ERG1-B, expression in the LC was also confirmed via in situ hybridization (Figure 1F–I). Moreover, ERG-positive cells were Tyrosine Hydroxylase (TH) positive, further confirming their expression in LC neurons (Figure 1J–M). Overall, these observations demonstrated that ERG-1A, ERG-1B, ERG-2 and ERG-3 channel types are expressed by LC neurons.

2.2. ERG Channels Regulate the Spontaneous Activity of LC Neurons

LC neurons in the pons were confined to the border of the IVth ventricle (Figure 2A,B), within an anatomical area that was readily identifiable for patch-clamp recordings from living brain slices imaged under infrared differential interference contrast microscopy. Moreover, the electrical properties of LC neurons recorded in brain slices were remarkably uniform [8], which further facilitated their recognition and recording. Slices were dissected from P40 ± 10-day-old mice and the electrical properties of LC neurons were assessed by means of whole-cell patch-clamp recordings in current-clamp mode [8]. LC neurons were spontaneously active (within the range of 0.5–5 Hz), displayed pacemaker-like firing, and possessed consistent action potential parameters. In particular, their resting membrane potentials oscillated between −32 mV and −55 mV, displayed input resistance of 366 ± 41 MΩ (n =12) and basal firing frequencies of 3.4 ± 0.5 Hz (n = 12). To assess the functional role of ERG channels in LC neurons, we used WAY-123,398 (WAY), an ERG channel blocker, the efficacy of which we had previously

reported in brain-slice recordings [20,29–31]. The electrophysiological properties of LC neurons modulated by ERG channels were analyzed under control conditions by perfusing the brain slices with a CSF and adding 10 µM WAY (final concentration in aCSF) to investigate the effects of channel block on the spontaneous discharge of these neurons and during a wash-out period. An enhancement of the spontaneous firing frequency was observed in LC neurons after the addition of WAY (Figure 3A, Table 1; WAY 188 ± 35, % of baseline vs. wash-out 109 ± 13.6, % of baseline $p < 0.05$; $n = 6$ neurons). There was no significant difference between the wash-out and baseline levels, indicating that this enhancement was reversed during drug wash-out. Figure 3B shows the effect of WAY on a representative LC neuron. WAY was able to almost double the firing frequency and cause an neuronal firing irregularity, which consisted of frequency fluctuations with unpredictable intervals (Figure 4D, raster plot).

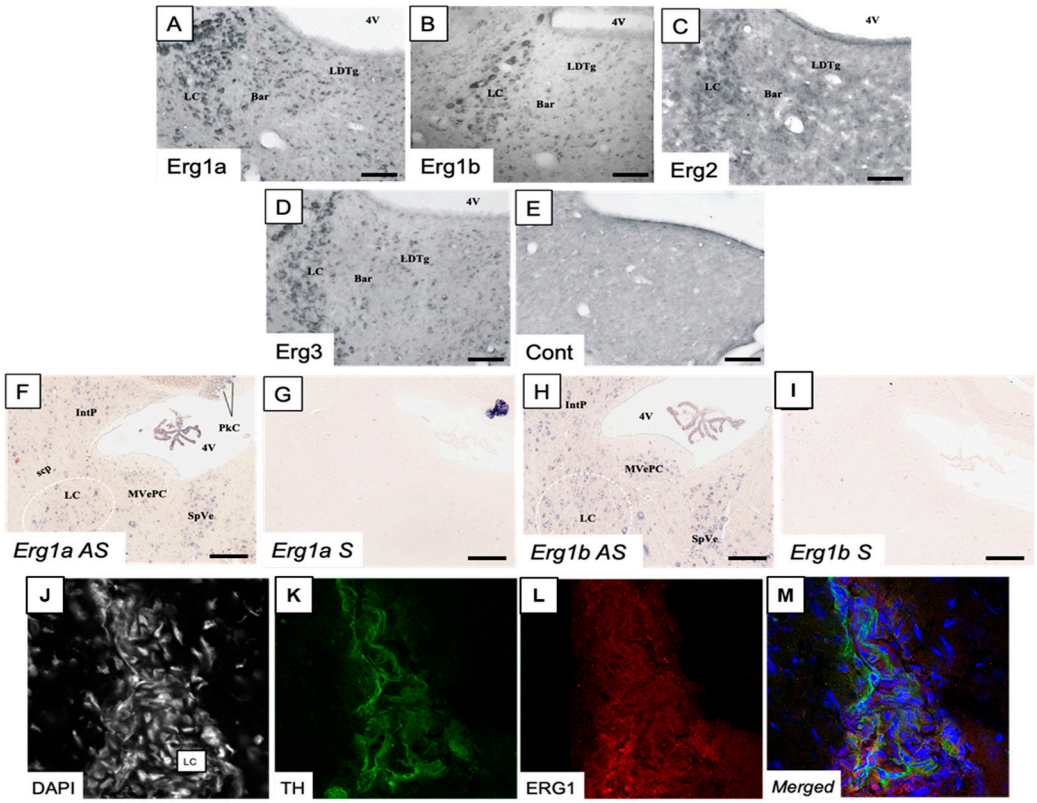

Figure 1. Expression of ERG1 channels in LC neurons. (**A**–**D**) Expression of Erg1a (**A**), Erg1b (**B**), Erg2 (**C**) and Erg3 (**D**) proteins in the LC and adjacent areas, as visualized through immunohistochemistry. (**E**) represents a stained section where the primary antibody was omitted. (**F**–**I**) Expression of *Erg1a* (**F**) and *Erg1b* (**H**) mRNAs in the LC and adjacent areas (sagittal sections), via non-radioactive in situ hybridization using anti-sense probes. Sections processed in parallel with sense probes (**G**,**I**) showed no signal. High magnification images of LC stained with the anti-TH (**K**) and anti-ERG1 (**L**) antibodies. Images of neurons stained with DAPI (**J**) and merged (**M**) are reported. Note that cells within the LC nucleus (indicated as LC) were heavily stained by the anti-TH specific antibody (green signal). Staining with anti-ERG1 antibody (red signal) was also present. Scale bars (**A**–**I**) = 100 µm, (**J**–**M**) image size is 185 × 185 µm. Abbreviations: 4V, 4th ventricle; Bar, Barrington's nucleus; IntP, interposed cerebellar nucleus, posterior part; LC, Locus coeruleus; LDTg, laterodorsal tegmental nucleus; MVePC, medial vestibular nucleus, parvicellular part; PkC, Purkinje cells; SpVe, spinal vestibular nucleus.

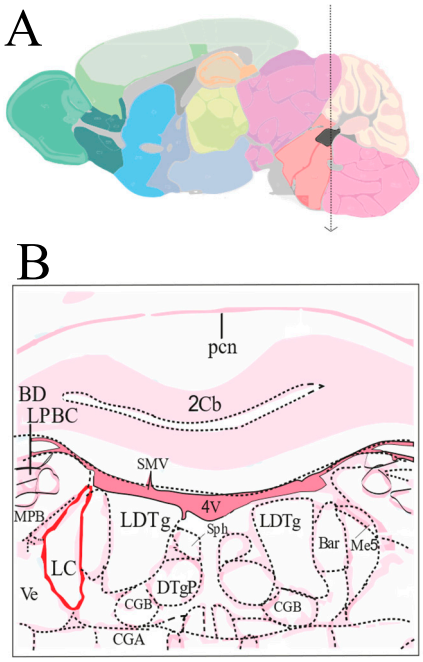

Figure 2. Anatomical localization of LC nucleus. (**A**) Sagittal section of the murine whole brain, each color distinguishes different regions in the brain, with black showing the localization of the LC nucleus in the pons of brainstem. (**B**) Cartoon showing the boundaries of the LC nucleus in red at the level of the Vth ventricle, compared to other surrounding structures in pink, where sections were dissected.

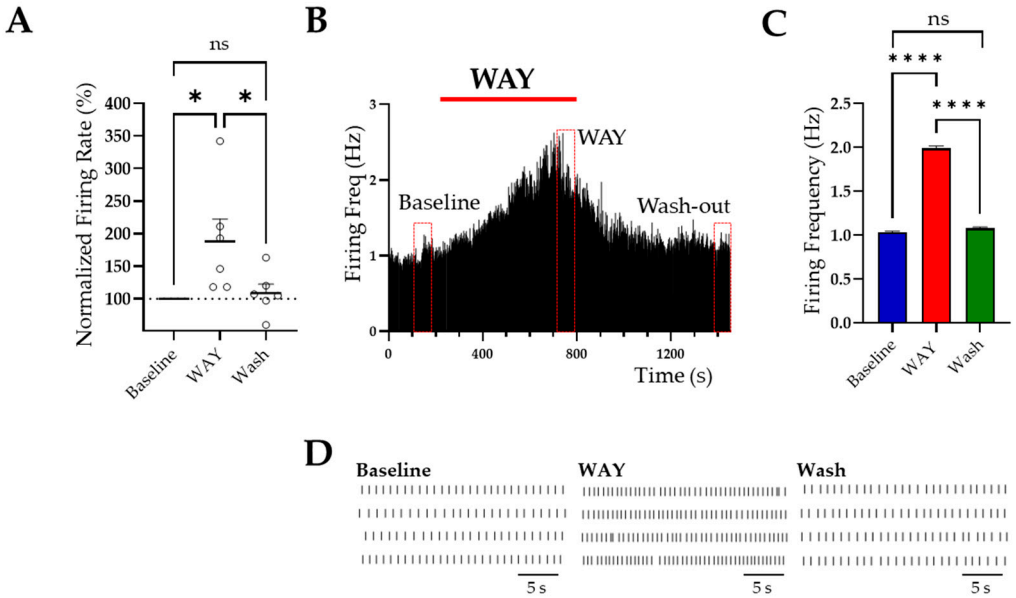

Figure 3. WAY increased LC neuron firing frequency. (**A**) Plot showing LC neuron firing rate (%) increased after WAY application and recovered back to baseline levels during the wash-out period. One-way ANOVA was performed on the mean of data points taken from a 60 s period representing the peak effect of each condition. * $p < 0.05$; $n = 6$ neurons each from a different mouse. (**B**) Firing frequency from a representative LC neuron. The firing frequency of a 60 s period in control/baseline conditions, during WAY application and during the wash-out. (**C**) Bar graph showing data from the neuron in (**B**). One-way ANOVA was performed on the mean data points enclosed by the red rectangles shown in (**B**); **** $p < 0.0001$. (**D**) Raster plots of the data shown in (**B**).

Table 1. Effects of WAY application on firing properties and firing pattern of LC neurons.

WAY-123,398 10 µM (*n* = 6 Neurons)			Wash-Out (*n* = 6 Neurons)		
Firing Freq [+]	ISI [+]	CV [+]	Firing Freq [+]	ISI [+]	CV [+]
188 ± 35 *	62 ± 10 *	124 ± 14	109 ± 14 *	102 ± 14.4	112 ± 10

[+] % of baseline ± SEM; percentage of variation in firing rate, ISI and CV during the application and wash-out of drug. The results represent the mean of 6 different recordings from 6 mice. * Significantly different from baseline $p < 0.05$.

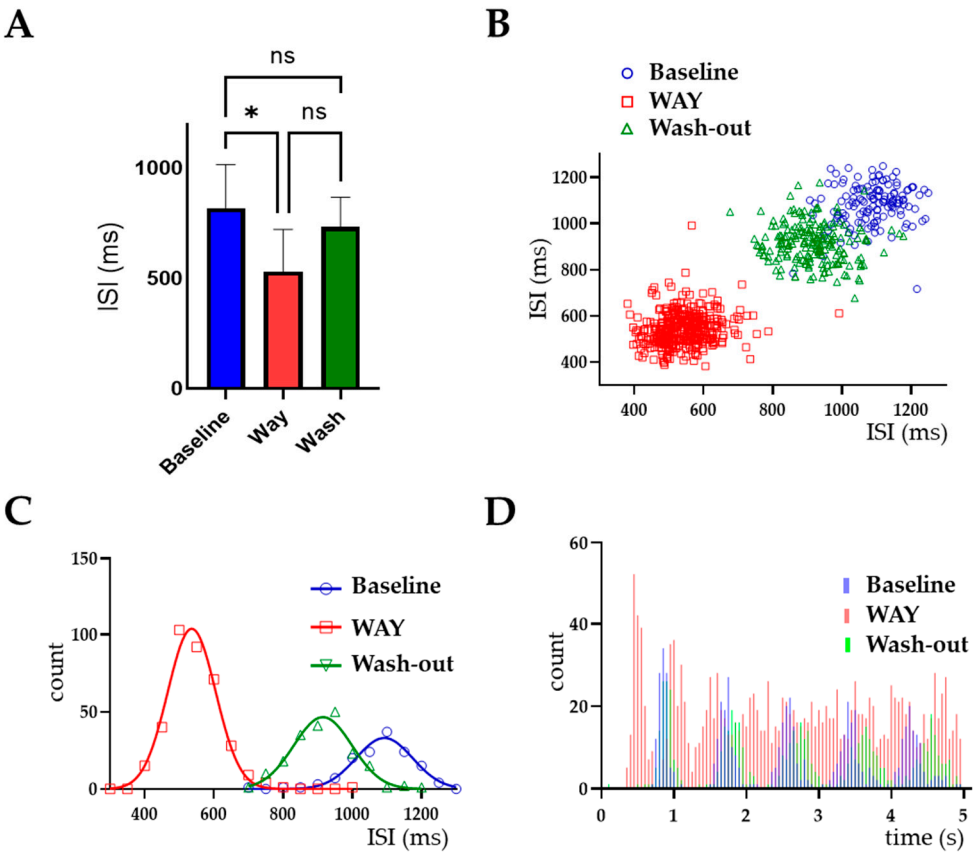

Figure 4. WAY alters LC neuronal firing pattern. (**A**) Bar graph showing a decrease in mean inter-spike interval (ISI) with WAY application (* $p < 0.05$, ns = no significant difference, $n = 6$), that was reversed by wash-out. (**B**–**D**) Representative data from a single neuron, showing ISI scatterplots (**B**), ISI distributions fitted with the Gaussian equation Y = Amplitude × exp(−0.5 × ((X-Mean)/SD)^2) (**C**) and ISI auto-correlograms (**D**) calculated in baseline conditions (blue), during WAY application (orange) and after drug wash-out (green), from a 200 s representative period of a single recording. Raw ISI values are plotted. The plots point out a regular firing pattern in the baseline and wash-out periods that is remarkably evidenced by the regular peaks in the ISI auto-correlograms. By contrast, a more irregular firing pattern of LC neurons during WAY application was clearly seen by the less defined peaks.

While there was no significant difference in the coefficient of variation (CV), the inter-spike interval (ISI) decreased following WAY application (baseline 819 ± 197 ms vs. WAY 531 ± 191 ms, one-way ANOVA, $p < 0.05$, $n = 6$, Figure 4A). Wash-out recovered the ISI back to 733 ± 135 ms, with no statistically significant difference between it and the baseline ($n = 6$, $p = 0.6$; Figure 4A, Table 1). The regular firing pattern of LC neurons recorded in control conditions was characterized by the well-defined cluster in the scatterplot (Figure 4B), the narrow bell-shaped distribution of the ISI histogram (Figure 4C) and the well-defined multiple peaks in the auto-correlogram (Figure 4D). The discharge irregularity brought about by WAY was demonstrated by the more dispersed cluster in the scatterplot (Figure 4B), and the flatter distribution with fewer peaks in the ISI auto-correlogram (Figure 4D).

3. Discussion

In this study, and for the first time, proof of the presence of ERG-1A, ERG-1B, ERG-2 and ERG-3 channel subunits in the LC was established. The widespread expression of ERG channels in the brain and in very critical regions, such as the LC, indicates the importance of this channel type in the regulation of CNS functions. The study, also for the first time, brings forth the channel's imperative role in regulating neuronal discharge patterns in LC neurons. Specifically, we reported in LC neurons a significant enhancement of spontaneous tonic firing frequency accompanied by an increase in firing irregularities after specific block of the ERG channels, indicating that ERG channels are a mechanistic tool that prevents increased firing rates and discharge irregularities in LC neurons.

Previous studies on other brain regions have shown that ERG channels variably affect neuronal excitability and firing frequency. ERG channel blockers increase [17,18,20,26] or decrease [32] firing frequency. They may cause or enhance spike-frequency adaptation [26], reduce spike-frequency adaptation, converting it to regular firing [17,18,20], or affect the resonance properties of neurons [20]. The variation may be due to differences in the characteristics of the areas and dynamic properties of the neurons, including the type of inputs impinging on the neuron and the resulting intracellular signaling cascades. Indeed, ERG channels are modulated by several intracellular signaling pathways that may mediate their role as regulators of excitability. In particular, protein kinase A and C inhibit ERG channel function by direct ERG subunit phosphorylation, suggesting that ERG channels, and, consequently, neuronal excitability, can be regulated by a variety of G-protein coupled receptors [33]. Notably, the stimulation of M_1 and M_2 muscarinic receptors activates PKC, and raises $[Ca^{2+}]_i$ and inhibits human ERG currents [34,35]. In the LC, acetylcholine induces increases in the neuronal firing rate, which is antagonized by the M_1 antagonist pirenzepine [36,37]. Similarly, activation of the metabotropic glutamate receptor mGluR1 in Purkinje cells and mitral/tufted cells of the olfactory bulb reduced ERG currents and increased firing frequency and excitability [35,38]. Intriguingly, mGluR1 receptors are expressed in LC neurons [33], where they may play a role in the enhancement of firing rate via ERG channel modulation.

LC neurons are intrinsic pacemakers that fire spontaneously in the absence of synaptic input. Recent optogenetic studies have confirmed that there is a variability in the LC neuronal firing rate and pattern that mediates the diverse behavioral functions associated with the LC [7,38]. For example, the LC's widespread innervation throughout the CNS allows for global brain arousal, and increases in LC neuronal firing rates are correlated with increased synchrony and arousal [39–41]. Moreover, different LC discharge rates are associated with different levels of arousal and anxiety states [7,39,40]. In the LC, increased tonic firing, such as that which we have observed with the ERG channel block, induces anxiety and aversive behaviors [42], whereas a decrease in LC tonic discharge rate is associated with a disengagement from the environment [6,43] and is evident, for instance, during slow-wave sleep. In contrast, there is discharge silence during REM sleep. During the arousal state, a moderate tonic firing is necessary for the occurrence of phasic burst firing in response to salient stimuli [44]. Unlike the 1–6 Hz continuous discharge in the tonic mode, in the phasic mode LC neurons synchronously fire in bursts of 10–15 Hz, permitting optimum performance and allowing for a shift in focus to task-related functions as well as to novel stimuli [6,45]. Excessive or insufficient tonic firing would impede phasic firing and its associated task performance. These electrophysiological observations indicate strongly that changes in the firing rate are involved in the transition between states of arousal and consciousness as well as moving from one stage of the sleep–wake cycle to another. While these findings bring forth LC firing patterns as a mechanism for the generation of different states and behaviors, we propose that ERG channels are important players behind the changes in, and/or maintenance of, firing rates. As such, it would be interesting to investigate ERG dysfunction in different anxiety, attention, and sleep disorders.

Many antipsychotic medications, such as *Haloperidol* and *Chlorpromazine*, are potent ERG channel inhibitors or blockers [16,46], indicating a possible association between altered ERG

activity and cognitive dysfunction. The antipsychotic effects of these medications are induced by blocking dopamine receptors. However, these medications also block ERG channels at similar therapeutic concentrations, thereby affecting neuronal excitability [16,18,46]. As such, an ERG channel blockade may contribute to the antipsychotic effect. Notably, in a human study, *Haloperidol* administration significantly improved memory performance, which was associated with increased LC activity [47]. On the other hand, antipsychotics, as well as antibiotics and antiemetics, that are known to inhibit or block ERG channels, can predispose certain individuals to *long QT syndrome* and cardiac arrhythmias due to the blockade of cardiac ERG channels. However, LC noradrenergic activation increases the heart rate and the adverse risks associated with tachycardia by depressing the activity of parasympathetic cardiac vagal neurons [48]. We propose that these drugs' blockage of the ERG channels in LC neurons alter their firing pattern and possibly change the heart rate, potentially enhancing the risk of cardiac arrhythmia. Thus, the potential role of ERG channels in the LC and the mechanisms of action of these medications would deserve further investigation.

There is evidence for the pathological role of ERG channels in the brain. The significant co-occurrence of epilepsy with *long QT syndrome* is noteworthy [49,50]. Furthermore, mutations in the *KCNH7* gene (ERG-3, Kv11.3) were associated with bipolar spectrum disorders [51,52]. The results of these studies have shed light on the possible role of ERG channel dysfunction in diseases involving the LC. The role of the LC in bringing about schizophrenia's cognitive symptoms has been recently emphasized with the observation that positive symptoms are consistent with hyperactivity of the LC noradrenergic system, while negative symptoms are consistent with a hypoactivity of this system [53]. Interestingly, ERG dysfunction and its associated disruption in neural firing has been implicated in schizophrenia [54,55]. ERG3 expression in schizophrenic hippocampi was 2.5-fold greater than ERG-1A, resulting in a rapidly deactivating K^+ current and a high-frequency, non-adapting firing pattern [54]. More importantly, an association between ERG mutations and schizophrenia has been established [54–57]. Finally, stress-initiated LC dysfunction has been proposed along with genetic susceptibility as being responsible for observed tonic- and phasic-firing imbalances that lead to schizophrenic dysfunctional network integration and cognitive deficits [54]. Are these schizophrenic LC firing imbalances and altered excitability a result of abnormal ERG currents? This question remains to be answered, and suggests a need for novel therapeutic investigation based on ERG-modulating agents.

LC's role in the prodromal or premotor stage of Parkinson's disease is well established [58]. In fact, LC cells show *αSyn* aggregation and *Lewy* pathology formation several years earlier than dopaminergic SN neurons' degeneration is apparent. In Parkinson's disease models, *αSyn* overexpression or *rotenone* exposure enhanced the spontaneous LC discharge frequency, which was associated with a marked decrease of after-hyperpolarization amplitude [58]. The small-conductance Ca^{2+}-activated K^+ (SK) channels were proposed as mediators of this enhancement. Interestingly, in Parkinsonian rats, ERG K^+ channel blockers reduced burst discharges and the firing frequency of subthalamic nucleus neurons, which led to an improvement in locomotor deficits, while the activators led to an increased burst mode and impaired motor function in normal rats [21]. Here, we propose that ERG channels reduced the mediators of the spontaneous firing rate in the LC. Therefore, it would be interesting to explore LC ERG channel dysfunction as a possible contributor to Parkinson and, more importantly, to explore the modulation of the LC ERG channel as a therapeutic option.

In conclusion, we reported the protein expression of ERG channels in mice LC nuclei and we presented electrophysiological data to confirm not only that they are functional, but that they play a key role in the LC neuronal discharge pattern. We presented ERG channels as essential means for the control of speed and stability of LC firing. The outcome of ERG channel activity on LC neuronal excitability may be a contributing mechanism towards LC's regulation of several physiological processes attributed to it. Furthermore, ERG K^+ channel dysfunction may constitute an important pathophysiological mechanism for disorders of the central nervous system associated with LC and the noradrenergic

system, and should be considered during pharmacotherapeutic interventions and vigilance. We anticipate that, in the near future, known neurological and psychiatric disorders will be shown to be largely attributed to ERG channel dysfunction in brain areas including the LC.

4. Materials and Methods

4.1. Immunohistochemistry

This study was carried out using brainstem tissue dissected from young (P10) and adult (P60) mice (C57BL/6J). This procedure was performed in accordance with national and international regulations, approved by the ethics committee, and compliant with ARRIVE guidelines. Mice were transcardially perfused with saline (0.9% *w*/*v* sodium chloride), followed by paraformaldehyde (Sigma, St. Louis, MO, USA; 4% *w*/*v*) in phosphate-buffered saline (PBS, 3.2 mM Na_2HPO_4, 0.5mM KH_2PO_4, 1.3 mM KCl, 135 mM NaCl, pH7.4) under terminal anesthesia induced by chloral hydrate (300 mg/kg *i.p.*). Brains were removed and post-fixed overnight at 4 °C in the same fixative, then soaked in 30% sucrose for cryoprotection. Brains were rapidly frozen and slices were obtained with a freezing cryostat at 30 µm thickness and collected in ice-cold PBS. Immunohistochemistry was performed as described previously [19]. The specificity of antibodies in recognizing ERG proteins in mouse brain-sections has been previously described [19]. Images were acquired with a Leica DMR light microscope equipped with a Leica DC200 digital camera, converted to greyscale, and adjusted for brightness and contrast using Adobe Photoshop (v.6.0; Abode Systems, San Jose, CA, USA). Each immunohistochemical experiment was repeated by using brainstem slices collected from three animals at both P10 and P60.

Immunofluorescence (IF) on cells was performed following the protocol previously described by Guasti et al., 2008 [19]. For IF on mice brains, the latter was kindly provided by Prof. Andrea Becchetti (Department of Biotechnology and Biosciences, University of Milano-Bicocca, Milano, Italy), snap frozen in liquid nitrogen and sectioned with a cryostat in 20 mm sections to localize the LC area. After 2 hours of blocking in PBS with 10% BSA, sections were incubated for a further 2 hours with anti-TH (Millipore) (diluted 1:10), followed by 1 hour incubation with antimouse Alexa Fluor 488 (Thermo Fisher Scientific). Incubation with poly-hERG1 was performed overnight (diluted 1:100) at 4 °C. Nuclei were stained with Hoechst (1:1000 in PBS, 45 minutes; Merck Sigma). Images were captured using a Nikon TE2000 confocal microscope, as described in Lottini, et al., 2021 [59].

4.2. Tight-Seal, Whole-Cell Recordings

This study was carried out using brainstem slices dissected from adult C57BL/6J male mice (P40 ± 10). Mice were decapitated after 30 min of deep chloral hydrate (4% in saline, intraperitoneal) anesthesia and the cranium was opened to expose the entire brain. The brain was rapidly removed and put into an ice-cold oxygenated solution of 2.5 mM KCl, 26.2 mM $NaHCO_3$, 1 mM NaH_2PO_4, 2 mM $MgSO_4$, 0.5 mM $CaCl_2$, 11 mM D-glucose, 238 mM sucrose, saturated with 95% O_2 and 5% CO_2, at pH 7.4. Coronal slices (220 µm thickness) were cut from the brainstem (submerged in the same ice-cold solution) using a Vibratome. Slices containing the LC were incubated at 30 °C for 30 min in *artificial cerebrospinal fluid* (aCSF) (125 mM NaCl, 2.5 mM KCl, 26 mM $NaHCO_3$, 1.25 mM NaH_2PO_4, 1 mM $MgCl_2$, 2.4 mM $CaCl_2$, 11 mM D-glucose, saturated with 95% O_2 and 5% CO_2, pH7.4) and were transferred to a recording chamber (500 µl volume). The slice was secured by means of a nylon mesh glued to a U-shaped platinum wire that totally submerged the tissue in a continuously flowing aCSF at a rate of 2.5 ml/min (warmed to 32 ± 1 °C). All neurons fired spontaneously at frequencies between 0.5 and 5 Hz (3.6 ± 1.1 Hz) when perfused with control aCSF (95% O_2 and 5% CO_2, pH7.4).

Patch-clamp recordings were performed from LC neurons under visual control (using Hamamatsu and Axioskop 2FS infrared optics) and were recorded in the current-clamp configuration using an EPC-9 amplifier and acquired with Patch Master software (HEKA Elektronik GmbH, Reutlingen, Germany). Patch glass pipettes (King Precision Glass, Claremont, CA, USA) were pulled in several stages to a tip with approximately 1 µm

outside diameter, had resistances of 3–5 MΩ and were filled with an intracellular solution containing 115 mM CH_3KO_4S, 20 mM KCl, 1.5 mM $MgCl_2$, 5 mM HEPES, 0.1 mM EGTA, 2 mM Mg-ATP, 0.5 Na-GTP and 10 mM $C_4H_{10}N_3O_5P$ (pH 7.4). The liquid junction potential was calculated to be approximately 10 mV (pipette negative relative to bath). All data were obtained using this solution and left uncorrected. After the seal formation (2–10 GΩ), a whole-cell configuration was obtained by further suction of the patch membrane (200–300 MΩ). Current-clamp recordings were performed after ≥10 min of stable seal formation and were analyzed only if action potential amplitudes were ≥80mV, resting membrane potentials oscillated between −30 and −50 mV and series resistance changed <20% throughout the entire recording period.

4.3. ERG Channels' Blockage

To assess the functional role of ERG channels in LC neurons, we used 10 μM WAY-123,398 ($C_{19}H_{25}N_5O_4S$) which belongs to the class III anti-arrhythmic agents that block all ERG channel types at this concentration, in a voltage-independent fashion [29,30]. WAY-123,398 was a generous gift from Dr. W. Spinelli, Wyeth-Ayerst Research, Princeton, NJ, USA. WAY-123,398 aliquots of stock solution (1mM) were prepared in distilled water and stored at −20 °C. The blocker was diluted to its final concentration in aCSF. A complete exchange of the bath solution in the recording chamber occurred in approximately 2 min.

4.4. Data Analysis and Statistical Evaluation

Action potential peaks were detected using a suitable voltage threshold on Clampfit v10.7 software (Molecular Devices, San Jose, CA, USA). The firing frequency, in Hz, and inter-spike intervals (ISI), in ms, were automatically extracted following peak detection. The coefficient of variation (CV), a measure of firing irregularity, was calculated as follows: CV = σ/μ. Firing regularity analysis was performed using a Spike2 software script (Cambridge Electronic Design, Cambridge, UK) developed by Dr. Massimo Pierucci: (a) ISI scatterplots were used to compare differences in consecutive ISI data points. A compact scatter indicated a regular firing pattern. (b) ISI histograms were prepared and visualized as a Gaussian least-square fit, to test for a normal or skewed distribution of the data points; the former indicated a regular firing pattern. (c) ISI auto-correlograms were used to test for regular correlated peaks that signified a regular firing pattern. All statistical analyses and graph plotting were performed with GraphPad Prism v9.1 (GraphPad software, CA, USA). A Kolmogorov–Smirnov test was carried out on each data set to test for a normal distribution of data. A parametric or non-parametric one-way ANOVA with multiple comparisons was subsequently performed to compare the means of datasets before and after drug application and during wash-out. Statistical tests were carried out using representative 60 s periods of the raw data. Data were presented as the mean ± SEM.

Author Contributions: Conceptualization, S.H., M.P., M.V. and M.C.D.; Validation, A.A., P.I. and M.P.; Formal Analysis, F.D. and S.H.; Investigation, S.H., C.D. and L.G.; Resources, M.C.D.; Data Curation, F.D. and F.M.H.; Writing—Original Draft Preparation, S.H. and M.C.D.; Writing—Review & Editing, P.I. and M.V.; Supervision, M.C.D.; Project Administration, M.C.D.; Funding Acquisition, M.P. and M.V. All authors have read and agreed to the published version of the manuscript.

Funding: This research was funded by the United Arab Emirates University (UAEU) under grant no. 31M468, 31M452, and 21M149, and by the Malta Council for Science and Technology (MCST) Research & Innovation R&I-2017-029T BooKind. This project was in part funded by The Alfred Mizzi Foundation through the RIDT, Malta, under grant no. E17L077, which was awarded to Prof. M. Valentino.

Institutional Review Board Statement: The animal study protocol was approved by the Institutional Ethics Committee of the University of Malta (protocol cell).

Informed Consent Statement: Not applicable.

Data Availability Statement: Data are available upon request to the corresponding author.

Acknowledgments: Massimo Pierucci is acknowledged for his support in software script editing for data analysis. We would like to acknowledge the AIRC Foundation. Safa Shehab from the Department of Human Anatomy, College of Medicine and Health Sciences, UAE University is kindly acknowledged for his valuable feedback on this study.

Conflicts of Interest: The authors declare no conflict of interest.

References

1. Van Egroo, M.; Koshmanova, E.; Vandewalle, G.; Jacobs, H.I.L. Importance of the locus coeruleus-norepinephrine system in sleep-wake regulation: Implications for aging and Alzheimer's disease. *Sleep Med. Rev.* **2022**, *62*, 101592. [CrossRef] [PubMed]
2. Borodovitsyna, O.; Tkaczynski, J.A.; Corbett, C.M.; Loweth, J.A.; Chandler, D.J. Ageand Sex-Dependent Changes in Locus Coeruleus Physiology and Anxiety-Like Behavior Following Acute Stressor Exposure. *Front. Behav. Neurosci.* **2022**, *16*, 808590. [CrossRef] [PubMed]
3. Dahl, M.J.; Mather, M.; Werkle-Bergner, M. Noradrenergic modulation of rhythmic neural activity shapes selective attention. *Trends Cogn. Sci.* **2022**, *26*, 38–52. [CrossRef]
4. Llorca-Torralba, M.; Camarena-Delgado, C.; Suárez-Pereira, I.; Bravo, L.; Mariscal, P.; Garcia-Partida, J.A.; López-Martín, C.; Wei, H.; Pertovaara, A.; Mico, J.A.; et al. Pain and depression comorbidity causes asymmetric plasticity in the locus coeruleus neurons. *Brain* **2022**, *145*, 154–167. [CrossRef] [PubMed]
5. James, T.; Kula, B.; Choi, S.; Khan, S.S.; Bekar, L.K.; Smith, N.A. Locus coeruleus in memory formation and Alzheimer's disease. *Eur. J. Neurosci.* **2021**, *54*, 6948–6959. [CrossRef]
6. Ross, J.A.; Van Bockstaele, E.J. The Locus Coeruleus- Norepinephrine System in Stress and Arousal: Unraveling Historical, Current, and Future Perspectives. *Front. Psychiatry* **2021**, *11*, 519. [CrossRef] [PubMed]
7. Uematsu, A.; Tan, B.Z.; Ycu, E.A.; Cuevas, J.S.; Koivumaa, J.; Junyent, F.; Kremer, E.; Witten, I.B.; Deisseroth, K.; Johansen, J.P. Modular organization of the brainstem noradrenaline system coordinates opposing learning states. *Nat. Neurosci.* **2017**, *20*, 1602–1611. [CrossRef]
8. D'Adamo, M.C.; Shang, L.; Imbrici, P.; Brown, S.D.; Pessia, M.; Tucker, S.J. Genetic inactivation of Kcnj16 identifies Kir5.1 as an im-portant determinant of neuronal PCO2/pH sensitivity. *J. Biol. Chem.* **2011**, *286*, 192–198. [CrossRef]
9. Filosa, J.A.; Dean, J.B.; Putnam, R.W. Role of intracellular and extracellular pH in the chemosensitive response of rat locus coeruleus neurones. *J. Physiol.* **2002**, *541*, 493–509. [CrossRef]
10. Masuko, S.; Nakajima, Y.; Nakajima, S.; Yamaguchi, K. Noradrenergic neurons from the locus ceruleus in dissociated cell culture: Culture methods, morphology, and electrophysiology. *J. Neurosci.* **1986**, *6*, 3229–3241. [CrossRef]
11. Forsythe, I.D.; Linsdell, P.; Stanfield, P.R. Unitary A-currents of rat locus coeruleus neurones grown in cell culture: Rectification caused by internal Mg^{2+} and Na^{+}. *J. Physiol.* **1992**, *451*, 553–583. [CrossRef] [PubMed]
12. Pineda, J.; Aghajanian, G. Carbon dioxide regulates the tonic activity of locus coeruleus neurons by modulating a proton- and polyamine-sensitive inward rectifier potassium current. *Neuroscience* **1997**, *77*, 723–743. [CrossRef] [PubMed]
13. Sausbier, U.; Sausbier, M.; Sailer, C.A.; Arntz, C.; Knaus, H.-G.; Neuhuber, W.; Ruth, P. Ca2+-activated K+ channels of the BK-type in the mouse brain. *Histochem. Cell Biol.* **2005**, *125*, 725–741. [CrossRef] [PubMed]
14. Filosa, J.A.; Putnam, R.W. Multiple targets of chemosensitive signaling in locus coeruleus neurons: Role of K+ and Ca2+ channels. *Am. J. Physiol. Cell Physiol.* **2003**, *284*, C145–C155. [CrossRef] [PubMed]
15. Imber, A.N.; Putnam, R.W. Postnatal development, and activation of L-type Ca2+ currents in locus coeruleus neurons: Implications for a role for Ca2+ in central chemosensitivity. *J. Appl. Physiol.* **2012**, *112*, 1715–1726. [CrossRef]
16. Bauer, C.K.; Schwarz, J.R. *Ether-à-go-go* K^{+} channels: Effective modulators of neuronal excitability. *J. Physiol.* **2018**, *596*, 769–783. [CrossRef]
17. Chiesa, N.; Rosati, B.; Arcangeli, A.; Olivotto, M.; Wanke, E. A novel role for HERG K+ channels: Spike-frequency adaptation. *J. Physiol.* **1997**, *501*, 313–318. [CrossRef]
18. Sacco, T.; Bruno, A.; Wanke, E.; Tempia, F. Functional Roles of an ERG Current Isolated in Cerebellar Purkinje Neurons. *J. Neurophysiol.* **2003**, *90*, 1817–1828. [CrossRef]
19. Guasti, L.; Cilia, E.; Crociani, O.; Hofmann, G.; Polvani, S.; Becchetti, A.; Wanke, E.; Tempia, F.; Arcangeli, A. Expression pattern of the ether-a-go-go-related (ERG) family proteins in the adult mouse central nervous system: Evidence for coassembly of dif-ferent subunits. *J. Comp. Neurol.* **2005**, *491*, 157–174. [CrossRef]
20. Pessia, M.; Servettini, I.; Panichi, R.; Guasti, L.; Grassi, S.; Arcangeli, A.; Wanke, E.; Pettorossi, V.E. ERG voltage-gated K^{+} channels regulate excitability and discharge dynamics of the medial vestibular nucleus neurones. *J. Physiol.* **2008**, *586*, 4877–4890. [CrossRef]
21. Huang, C.-S.; Wang, G.-H.; Tai, C.-H.; Hu, C.-C.; Yang, Y.-C. Antiarrhythmics cure brain arrhythmia: The imperativeness of subthalamic ERG K^{+} channels in parkinsonian discharges. *Sci. Adv.* **2017**, *3*, e1602272. [CrossRef] [PubMed]
22. Sanguinetti, M.C.; Tristani-Firouzi, M. hERG potassium channels and cardiac arrhythmia. *Nature* **2006**, *440*, 463–469. [CrossRef] [PubMed]
23. Vandenberg, J.I.; Perry, M.D.; Perrin, M.J.; Mann, S.A.; Ke, Y.; Hill, A.P. hERG K+ channels: Structure, function, and clinical significance. *Physiol. Rev.* **2012**, *92*, 1393–1478. [CrossRef] [PubMed]

24. Furlan, F.; Taccola, G.; Grandolfo, M.; Guasti, L.; Arcangeli, A.; Nistri, A.; Ballerini, L.; Guasti, L. ERG Conductance Expression Modulates the Excitability of Ventral Horn GABAergic Interneurons That Control Rhythmic Oscillations in the Developing Mouse Spinal Cord. *J. Neurosci.* **2007**, *27*, 919–928. [CrossRef]
25. Hagendorf, S.; Fluegge, D.; Engelhardt, C.; Spehr, M. Homeostatic Control of Sensory Output in Basal Vomeronasal Neurons: Activity-Dependent Expression of Ether-à-Go-Go-Related Gene Potassium Channels. *J. Neurosci.* **2009**, *29*, 206–221. [CrossRef]
26. Ji, H.; Tucker, K.R.; Putzier, I.; Huertas, M.A.; Horn, J.P.; Canavier, C.C.; Levitan, E.S.; Shepard, P.D. Functional characterization of ether-à-go-go-related gene potassium channels in midbrain dopamine neurons—Implications for a role in depolarization block. *Eur. J. Neurosci.* **2012**, *36*, 2906–2916. [CrossRef]
27. Saganich, M.J.; Machado, E.; Rudy, B. Differential Expression of Genes Encoding Subthreshold-Operating Voltage-Gated K^+ Channels in Brain. *J. Neurosci.* **2001**, *21*, 4609–4624. [CrossRef]
28. Papa, M.; Boscia, F.; Canitano, A.; Castaldo, P.; Sellitti, S.; Annunziato, L.; Taglialatela, M. Expression pattern of the ether-a-gogo-related (ERG) k+ channel-encoding genes ERG1, ERG2, and ERG3 in the adult rat central nervous system. *J. Comp. Neurol.* **2003**, *466*, 119–135. [CrossRef]
29. Spinelli, W.; Moubarak, I.F.; Parsons, R.W.; Colatsky, T.J. Cellular electrophysiology of WAY-123,398, a new class III antiarrhythmic agent: Specificity of IK block and lack of reverse use dependence in cat ventricular myocytes. *Cardiovasc. Res.* **1993**, *27*, 1580–1591. [CrossRef]
30. Faravelli, L.; Arcangeli, A.; Olivotto, M.; Wanke, E. A HERG-like K+ channel in rat F-11 DRG cell line: Pharmacological identification and biophysical characterization. *J. Physiol.* **1996**, *496*, 13–23. [CrossRef]
31. Williams, J.T.; North, A.R. Opiate-receptor interactions on single locus coeruleus neurones. *Mol. Pharmacol.* **1984**, *26*, 489–497. [PubMed]
32. Cui, E.D.; Strowbridge, B.W. Modulation of Ether-à-Go-Go Related Gene (ERG) Current Governs Intrinsic Persistent Activity in Rodent Neocortical Pyramidal Cells. *J. Neurosci.* **2017**, *38*, 423–440. [CrossRef] [PubMed]
33. Noriega, N.C.; Garyfallou, V.T.; Kohama, S.G.; Urbanski, H.F. Glutamate receptor subunit expression in the rhesus macaque locus coeruleus. *Brain Res.* **2007**, *1173*, 53–65. [CrossRef] [PubMed]
34. Cockerill, S.L.; Tobin, A.B.; Torrecilla, I.; Willars, G.B.; Standen, N.B.; Mitcheson, J. Modulation of hERG potassium currents in HEK-293 cells by protein kinase C. Evidence for direct phosphorylation of pore forming subunits. *J. Physiol.* **2007**, *581*, 479–493. [CrossRef] [PubMed]
35. Hirdes, W.; Horowitz, L.F.; Hille, B. Muscarinic modulation of erg potassium current. *J. Physiol.* **2004**, *559*, 67–84. [CrossRef]
36. Egan, T.; North, R. Acetylcholine acts on m2-muscarinic receptors to excite rat locus coeruleus neurones. *J. Cereb. Blood Flow Metab.* **1985**, *85*, 733–735. [CrossRef]
37. Freedman, S.B.; Beer, M.S.; Harley, E.A. Muscarinic M1, M2 receptor binding. relationship with functional efficacy. *Eur. J. Pharmacol.* **1988**, *156*, 133. [CrossRef]
38. Niculescu, D.; Hirdes, W.; Hornig, S.; Pongs, O.; Schwarz, J.R. Erg Potassium Currents of Neonatal Mouse Purkinje Cells Exhibit Fast Gating Kinetics and Are Inhibited by mGluR1 Activation. *J. Neurosci.* **2013**, *33*, 16729–16740. [CrossRef]
39. Carter, M.; Yizhar, O.; Chikahisa, S.; Nguyen, H.; Adamantidis, A.; Nishino, S.; Deisseroth, K.; De Lecea, L. Tuning arousal with optogenetic modulation of locus coeruleus neurons. *Nat. Neurosci.* **2010**, *13*, 1526–1533. [CrossRef]
40. Poe, G.R.; Foote, S.; Eschenko, O.; Johansen, J.P.; Bouret, S.; Aston-Jones, G.; Harley, C.W.; Manahan-Vaughan, D.; Weinshenker, D.; Valentino, R.; et al. Locus coeruleus: A new look at the blue spot. *Nat. Rev. Neurosci.* **2020**, *21*, 644–659. [CrossRef]
41. Alvarez, V.A.; Chow, C.C.; Van Bockstaele, E.J.; Williams, J.T. Frequency-dependent synchrony in locus ceruleus: Role of electrotonic coupling. *Proc. Natl. Acad. Sci. USA* **2002**, *99*, 4032–4036. [CrossRef] [PubMed]
42. McCall, J.G.; Al-Hasani, R.; Siuda, E.R.; Hong, D.Y.; Norris, A.J.; Ford, C.P.; Bruchas, M.R. CRH Engagement of the Locus Coeruleus Noradrenergic System Mediates Stress-Induced Anxiety. *Neuron* **2015**, *87*, 605–620. [CrossRef]
43. Aston-Jones, G.; Cohen, J.D. An Integrative Theory of Locus Coeruleus-Norepinephrine Function: Adaptive Gain and Optimal Performance. *Annu. Rev. Neurosci.* **2005**, *28*, 403–450. [CrossRef] [PubMed]
44. Howells, F.M.; Stein, D.; Russell, V.A. Synergistic tonic and phasic activity of the locus coeruleus norepinephrine (LC-NE) arousal system is required for optimal attentional performance. *Metab. Brain Dis.* **2012**, *27*, 267–274. [CrossRef]
45. Janitzky, K. Impaired Phasic Discharge of Locus Coeruleus Neurons Based on Persistent High Tonic Discharge—A New Hypothesis with Potential Implications for Neurodegenerative Diseases. *Front. Neurol.* **2020**, *11*, 371. [CrossRef]
46. Wang, Z.-J.; Soohoo, S.; Tiwari, P.B.; Piszczek, G.; Brelidze, T.I. Chlorpromazine binding to the PAS domains uncovers the effect of ligand modulation on EAG channel activity. *J. Biol. Chem.* **2020**, *295*, 4114–4123. [CrossRef] [PubMed]
47. Clos, M.; Bunzeck, N.; Sommer, T. Dopamine is a double-edged sword: Dopaminergic modulation enhances memory retrieval performance but impairs metacognition. *Neuropsychopharmacology* **2019**, *44*, 555–563. [CrossRef] [PubMed]
48. Wang, X.; Piñol, R.A.; Byrne, P.; Mendelowitz, D. Optogenetic stimulation of locus ceruleus neurons augments inhibitory transmission to parasympathetic cardiac vagal neurons via activation of brainstem α1 and β1 receptors. *J. Neurosci.* **2014**, *34*, 6182–6189. [CrossRef] [PubMed]
49. Johnson, J.N.; Hofman, N.; Haglund, C.M.; Cascino, G.D.; Wilde, A.; Ackerman, M.J. Identification of a possible pathogenic link between congenital long QT syndrome and epilepsy. *Neurology* **2008**, *72*, 224–231. [CrossRef]
50. Omichi, C.; Momose, Y.; Kitahara, S. Congenital long QT syndrome presenting with a history of epilepsy: Misdiagnosis or rela-tionship between channelopathies of the heart and brain? *Epilepsia* **2009**, *51*, 289–292. [CrossRef]

51. Kuo, P.H.; Chuang, L.C.; Liu, J.R.; Liu, C.M.; Huang, M.C.; Lin, S.K.; Sunny Sun, H.; Hsieh, M.H.; Hung, H.; Lu, R.B. Identification of novel loci for bipolar I disorder in a multi-stage genome-wide association study. *Prog. Neuropsychopharmacol. Biol. Psychiatry* **2014**, *51*, 58–64. [CrossRef] [PubMed]
52. Strauss, K.A.; Markx, S.; Georgi, B.; Paul, S.M.; Jinks, R.N.; Hoshi, T.; McDonald, A.; First, M.B.; Liu, W.; Benkert, A.R.; et al. A population-based study of KCNH7 p.Arg394His and bipolar spectrum disorder. *Hum. Mol. Genet.* **2014**, *23*, 6395–6406. [CrossRef] [PubMed]
53. Mäki-Marttunen, V.; Andreassen, O.A.; Espeseth, T. The role of norepinephrine in the pathophysiology of schizophrenia. *Neurosci. Biobehav. Rev.* **2020**, *118*, 298–314. [CrossRef] [PubMed]
54. Huffaker, S.J.; Chen, J.; Nicodemus, K.K.; Sambataro, F.; Yang, F.; Mattay, V.; Lipska, B.K.; Hyde, T.M.; Song, J.; Rujescu, D.; et al. A primate-specific, brain isoform of KCNH2 affects cortical physiology, cognition, neuronal repolarization and risk of schizophrenia. *Nat. Med.* **2009**, *15*, 509–518. [CrossRef]
55. Atalar, F.; Acuner, T.T.; Cine, N.; Oncu, F.; Yesilbursa, D.; Ozbek, U.; Turkcan, S. Two four-marker haplotypes on 7q36.1 region indicate that the potassium channel gene HERG1 (KCNH2, Kv11.1) is related to schizophrenia: A case control study. *Behav. Brain Funct.* **2010**, *6*, 27. [CrossRef]
56. Apud, J.A.; Zhang, F.; Decot, H.; Bigos, K.L.; Weinberger, D.R. Genetic Variation in *KCNH2* Associated with Expression in the Brain of a Unique hERG Isoform Modulates Treatment Response in Patients with Schizophrenia. *Am. J. Psychiatry* **2012**, *169*, 725–734. [CrossRef]
57. Hashimoto, R.; Ohi, K.; Yasuda, Y.; Fukumoto, M.; Yamamori, H.; Kamino, K.; Morihara, T.; Iwase, M.; Kazui, H.; Takeda, M. The *KCNH2* gene is associated with neurocognition and the risk of schizophrenia. *World J. Biol. Psychiatry* **2013**, *14*, 114–120. [CrossRef]
58. Matschke, L.A.; Komadowski, M.A.; Stöhr, A.; Lee, B.; Henrich, M.T.; Griesbach, M.; Rinné, S.; Geibl, F.F.; Chiu, W.-H.; Koprich, J.B.; et al. Enhanced firing of locus coeruleus neurons and SK channel dysfunction are conserved in distinct models of prodromal Parkinson's disease. *Sci. Rep.* **2022**, *12*, 1–14. [CrossRef]
59. Lottini, T.; Iorio, J.; Lastraioli, E.; Carraresi, L.; Duranti, C.; Sala, C.; Armenio, M.; Noci, I.; Pillozzi, S.; Arcangeli, A. Transgenic mice overexpressing the LH receptor in the female reproductive system spontaneously develop endometrial tumour masses. *Sci. Rep.* **2021**, *11*, 8847. [CrossRef]